

Computational evaluation of pK_a for oxygenated side chain containing amino acids interacting with Aluminum

J. I. Mujika · J. M. Ugalde · X. Lopez

Received: 29 June 2010 / Accepted: 26 August 2010 / Published online: 14 September 2010
© Springer-Verlag 2010

Abstract The acidity of oxygen containing amino acids (Asp, Tyr, Ser, Thr) and the chemically analogue S-containing Cys was investigated using quantum mechanical methods when these amino acids interact with Al(III). The pK_a values of these residues were determined calculating the free energy of a proton transfer reaction from the metal-bound amino acid to a reference molecule, a water molecule interacting with the cation. In addition, for comparison, since Al(III) can replace Mg(II) in certain proteins, the acidity of these O-containing amino acid was also computed when they interact with Mg(II). All calculations were carried out combining the B3LYP density function method with the polarizable continuum PCM model. Our results confirm that the second solvation sphere water molecules must explicitly be included for an accurate description of interaction between the solute and the solvent. The computed pK_a values show that the acidity of all amino acids is enhanced when they interact with both cations. However, the pK_a values are significantly lower with Al(III) than with Mg(II). This difference in the acidity may lead to drastic chemical changes in proteins where Al(III) substitutes Mg(II). The present work allows to quantify the acidity shift of the title amino acids due to the influence of Al(III) and provides a valuable information for a better understanding of its biological consequences.

Keywords Aluminum · Acidity · Amino acid

Published as part of the special issue celebrating theoretical and computational chemistry in Spain.

J. I. Mujika · J. M. Ugalde · X. Lopez (✉)
Kimika Fakultatea, Euskal Herriko Unibertsitatea and Donostia
International Physics Center (DIPC), P.K. 1072,
20080 Donostia, Euskadi, Spain
e-mail: xabier.lopez@ehu.es

1 Introduction

Al(III) is a non-essential element that has been introduced in the living systems mainly due to human intervention [1]. The consequences of aluminum in human body is still uncertain, and its toxicity remains unclear. Nevertheless, aluminum has been involved in diseases such as dialysis dementia, or some renal bone diseases. Aluminum has been also related with Alzheimer disease, although the connection between aluminum uptake and development of this neurodegenerative diseases is still highly speculative [2]. Al(III) can interact with small molecules (citrate) and proteins (albumin and transferrin) in serum. The iron transporter transferrin is the main protein binding aluminum, and this interaction increases its bioavailability within the cell. On the other hand, Al(III) is seen to enter and permanently occupy binding sites which in healthy systems are served by other metal cations with specific binding and charge properties [3]. Mg(II) seems to be one of the most affected cations, since the two cations are similar in size, which is a dominant factor over the charge identity in terms of metal ion competition [4, 5]. For instance, some authors point out the substitution of Mg(II) by Al(III) in various binding sites as one of the causes of neurodegenerative diseases, such as Alzheimer [3, 6]. Al(III) has been seen to be able to alter a myriad of enzymes, as the hexokinase [7, 8], phosphofructokinase [9], acetylcholinesterase [10] or glutamate dehydrogenase [11]. Hexokinase, for instance, catalyzes the phosphorylation of glucose to glucose 6-phosphate by using Mg-ATP as a cofactor [12], and the uptake of Al(III) inhibits the normal activity of this enzyme [7, 8].

The increasing number of roles discovered for Al(III) in physiological processes demands an understanding of how Al(III) interacts with compounds in biological

systems, and how this interaction can change fundamental chemical properties of the interacting ligands. Metal ions are present in one-third of enzymes found in the nature. Numerous cations interact with proteins, and the broad type of features presented by the metals allow them to play a wide variety of roles, going from keeping the structure of the protein, to catalyze reactions. The inclusion of a trivalent cation such as Al(III) can alter the structure of a given metal site, and therefore, alter its function. A particular important aspect of Al(III) interaction with amino acids is the shift that can provoke in the acidity of key residues that form the active site. This could lead to an alteration of the protonation state of residues directly coordinated to Al(III), with the concomitant effects on the structure and activity of a given metalloenzyme. In addition, the determination of the shift in pK_a 's could shed light on the type of chemical species that Al(III) can form at physiological pH values within biological environments. In the present paper, we address this question through the theoretical evaluation of the shift in the pK_a of selected amino acids, mainly oxygen containing ones, when interacting with Al(III).

Computationally, the evaluation of a pK_a is not exempt from difficulty, and diverse approaches have been employed for an accurate evaluation of pK_a , which are summarized in several reviews [13, 14]. Several works have been published estimating the absolute pK_a of wide variety of molecules with reasonable success [15, 16, 17, 18]. In principle, the evaluation of an absolute pK_a would require the accurate estimation of the solvation free energy of H^+ . However, depending on the experiment, the solvation energy of H^+ can differ in ca. 5 kcal/mol, which may suppose deviation of 3 units in the final pK_a value. An alternative of the absolute or direct evaluation of pK_a is the evaluation of a relative pK_a with respect to a molecule, for which the pK_a is experimentally known. Thus, one considers the deprotonation of the acidic group as a proton transfer to a second molecule, preferably a water molecule. This strategy avoids the treatment of the solvation energy of proton, and it has been employed in many studies with satisfactory results [19, 20, 21, 22].

On the other hand, metallic hydrated cations pose specific challenges. For instance, the inclusion of a highly charged cation induces charge transfer between the metal center and the solvent. In several studies, it has been claimed that the implicit continuum models describe poorly this short-range interaction [23]. As an alternative, the inclusion of explicit water molecules in the outer solvation sphere yields improved results [24, 25]. Regarding aluminum, Bickmore et al. [26] employed bond-valence methods to determine the acidity of several reactions, among them the deprotonation of a Al(III)-bound water molecule. The authors obtained a value of

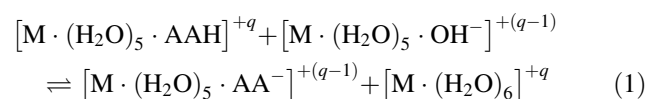
4.97, in very good agreement with the experimental value of 5.0 [27]. Yang et al. [28] studied the hydrolysis of aluminum characterizing the different structures upon water molecule deprotonation using density function theory. They defined a supermolecule including explicit water molecules for the second hydration sphere and compared pK_a values using the absolute and relative methods. The results indicate that the relative method is more appropriate for the first hydrolysis reaction, predicting a pK_a value of 4.6. However, little is known about the change in acidity for amino acids, due to their interaction with Al(III). Thus, in the present work, we determine the pK_a value for the most relevant oxygen-containing ligands that interacts with Al(III). To do so, their relative pK_a 's are calculated with respect to a metal-bound water molecule, for which its experimental pK_a value is well known. In addition, we also provide comparison of these shifts in pK_a with respect to the effect of another metal cation of similar size but lower charge, Mg(II), that has been pointed out as a possible target for Al(III) substitution due to size similarity [29].

After a brief description of the methodology followed in this study (Sect. 2), in Sect. 3 the results for pK_a values of Al(III)- and Mg(II)-bound oxygenated side chain containing amino acids are presented. Finally, a brief discussion of them are included in Sect. 4.

2 Computational details

2.1 pK_a calculation

The pK_a values of four oxygen-containing amino acids (aspartic acid, tyrosine, serine and threonine) and of the sulfur-containing ligand cysteine were determined interacting with two cations: Al(III) and Mg(II). To do so, the free energy in solution (ΔG_{aq}) for the reaction of proton transfer to a hydroxide ion coordinated to the metal was evaluated, that is:



where M stands for the cation (Al(III) or Mg(II)), and AAH and AA^- the protonated and unprotonated states for O-containing acidic amino acid. Phenol/phenolate, acetic acid/acetate, methanol/methoxide, ethanol/ethoxide and methylthiol/methylthiolate were used to represent the deprotonated/protonated side chains of tyrosine, aspartic acid, serine, threonine and cysteine, respectively. The q term denotes the charge of each cation [+3 for Al(III) and +2 for Mg(II)]. The pK_a of AAH ligand is then calculated as:

$$\text{p}K_a = \frac{\Delta G_{\text{aq.}}}{\ln_{10}RT} + \text{p}K_a^{\text{Ref}}(\text{exp.}) \quad (2)$$

where $\Delta G_{\text{aq.}}$ is calculated from Eq. 1 and $\text{p}K_a^{\text{Ref}}(\text{exp.})$ is the experimental $\text{p}K_a$ of the water molecule interacting with the cation. With this scheme, the relative $\text{p}K_a$ value is evaluated instead of the absolute $\text{p}K_a$, what avoids the need to deal with the proton solvation free energy. This protocol requires the choice of a similar reference molecule with a well-determined experimental $\text{p}K_a$, and therefore a water molecule interacting with the cation was chosen as this reference molecule (see Fig. 2) because: (1) water is an oxygen containing ligand, and in this sense, shows chemical similarities with the ligands to be studied, (2) the experimental $\text{p}K_a$ of a water molecule coordinated to Mg(II) and Al(III) is known ($\text{p}K_a = 12.4$ for the former and $\text{p}K_a = 5.0$ for the later), (3) the number of charged species is conserved in both sides of the chemical equation for which the free energy difference is calculated. With this protocol, a proper cancelation of errors is expected at both sides of Eq. 1. This protocol to evaluate $\text{p}K_a$'s was previously used by the authors for phosphoranes [30] and amides [31] obtaining successful results.

2.2 Ab-initio calculations

All geometrical optimizations were carried out in gas phase using the Gaussian 03 suite of programs [32] employing B3LYP functional [33, 34, 35, 36] in conjunction with the 6-31++g(d,p) basis set. The electronic energy was refined by single-point energy calculations at B3LYP/6-311++G(3df,2p). To confirm that the optimized structures were minima on the potential energy surfaces, frequency calculations were done at the same level of theory. The frequencies were then used to evaluate the zero-point vibrational energy (ZPVE) and the thermal ($T = 298$ K) vibrational corrections to the enthalpy and Gibbs free energy in the harmonic oscillator approximation. To calculate the entropy, the different contributions to the partition function were evaluated using the standard expressions for an ideal gas in the canonical ensemble and the harmonic oscillator and rigid rotor approximation. Thus, the final gas-phase enthalpy and free energy were obtained from the B3LYP/6-311++G(3df,2p) electronic energy and the enthalpic and entropic corrections evaluated at the B3LYP/6-31++G(d,p) level.

Solvation free energies at the gas-phase B3LYP/6-31++G(d,p) geometries were estimated with the polarizable continuum model (PCM) approach [37, 38, 39, 40]. The united atom Hartree-Fock (UAHF) set of atomic radii was used to define the cavity. These radii have been optimized with the HF/6-31G(d) wave function to give

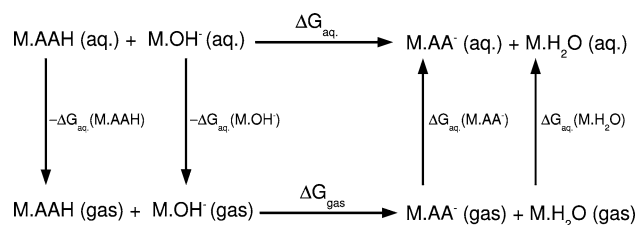
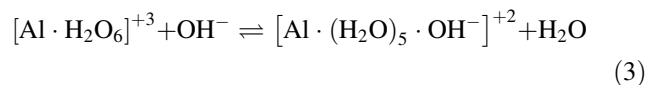


Fig. 1 Thermodynamic cycle used to evaluate the reaction free energy in solution ($\Delta G_{\text{aq.}}$) of Eq. 2

accurate solvation free energies of a dataset of anionic/cationic and neutral organic and inorganic molecules [38]. Therefore, the HF/6-31G(d) level of theory was chosen to represent the solute. To obtain the relative energy of each complex in solution, the contributions of solvation were added to the corresponding gas-phase relative energies. The thermodynamic cycle shown in Fig. 1 was employed to evaluate the relative free energies in aqueous solvent ($\Delta G_{\text{aq.}}$) for Eq. 2.

2.3 Importance of second solvation sphere

As it was pointed out in the Introduction section, inaccuracies of the continuum models for describing the strong hydrogen bonds of the first solvation shell around ions are expected. In order to further investigate this point and provide a sufficiently accurate model for aluminum coordination, two scenarios were defined: (1) consider aluminum and only its first solvation sphere, or (2) second sphere water molecules are also included. For both systems, the $\text{p}K_a$ of a water molecule interacting with Al(III) was determined according to the reaction:



taken into account the experimental $\text{p}K_a$ of 15.7 for a water molecule.

First, only the first solvation sphere was included in the quantum calculation, that is, Al(III) and six water molecules for $[\text{Al} \cdot (\text{H}_2\text{O})_6]^{+3}$, and a hydroxide ion and five water molecules for $[\text{Al} \cdot (\text{H}_2\text{O})_5 \cdot \text{OH}^-]^{+2}$. In both structures, Al(III) presents an octahedral arrangement. Thus, the interaction between the solute and the solvent was treated implicitly with the continuum PCM model, at the level of theory described in Computational Details. A $\text{p}K_a$ value of 18.6 was computed, far away from the experimental value of 5.0. As it has been pointed out in several studies, this error can be attributed to an inadequate description of short-range interaction by implicit solvent methods [23]. In order to verify this point, the proton affinity (PA) for a free OH^- was calculated as $\text{PA} = -\Delta H = -\Delta E_{\text{gas-phase}} + RT$, where ΔE

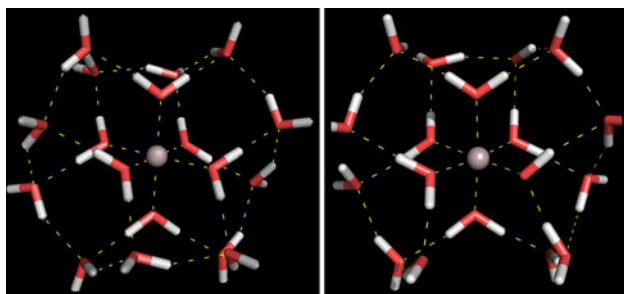


Fig. 2 B3LYP/6-31++G(d,p) optimized structures of $[\text{Al}(\text{H}_2\text{O})_6 \cdot 12\text{H}_2\text{O}]^{+3}$ and $[\text{Al}(\text{OH}^-)(\text{H}_2\text{O})_5 \cdot 12\text{H}_2\text{O}]^{+2}$ complexes, employed as reference to evaluate the pK_a of Al(III)-bound amino acids according to Eq. 2. Analogous complexes were characterized with Mg(II)

was determined as the difference in electronic energy between H_2O and OH^- in gas-phase. The calculated PA for a free OH^- is 1634.7 kJ/mol, in excellent agreement with the experimental value of 1635 kJ/mol [41]. From this result, it can be inferred that the origin of the error comes from a poor description of the Al(III)-water complex.

Therefore, the second solvation sphere of Al(III) was explicitly treated by including 12 explicit water molecules in the $[\text{Al} \cdot (\text{H}_2\text{O})_6]^{+3}$ and $[\text{Al} \cdot (\text{H}_2\text{O})_5 \cdot \text{OH}^-]^{+2}$ complexes (see Fig. 2). A similar supermolecule was previously characterized for hydrated Al(III) complex by Yang et al. [28] The new system leads to a considerable improvement of the calculated pK_a . Now, a value of 4.6 is obtained, in concordance with the 4.6 value calculated by Yang et al. [28] using a different methodology, and in very good agreement with the experimental value of 5.0 [27]. Thus, these calculations confirm the importance to treat properly the short-range interaction between the metal and solvent, by including explicitly the second solvation sphere, while the long-range interaction are correctly described by the continuum model. Hence, in all calculations carried out to estimate the pK_a values of amino acids the second solvation sphere was explicitly included in the different complexes characterized.

3 Results

Theoretical pK_a values were estimated for the Al(III)-complexes shown in Fig. 3. The solvation free energy (ΔG_{aq}) was determined for the proton transfer described in reaction 1. All $\text{Al} \cdot (\text{H}_2\text{O})_5\text{AAH}$ structures present an octahedral coordination. The deprotonation of the ligand leads to the $\text{M} \cdot (\text{H}_2\text{O})_5 \cdot \text{AA}^-$ structure, which keeps the octahedral conformation. In all complexes characterized, explicit water molecules are included in the second hydration sphere (see below).

3.1 Aluminum complexes

3.1.1 Structures

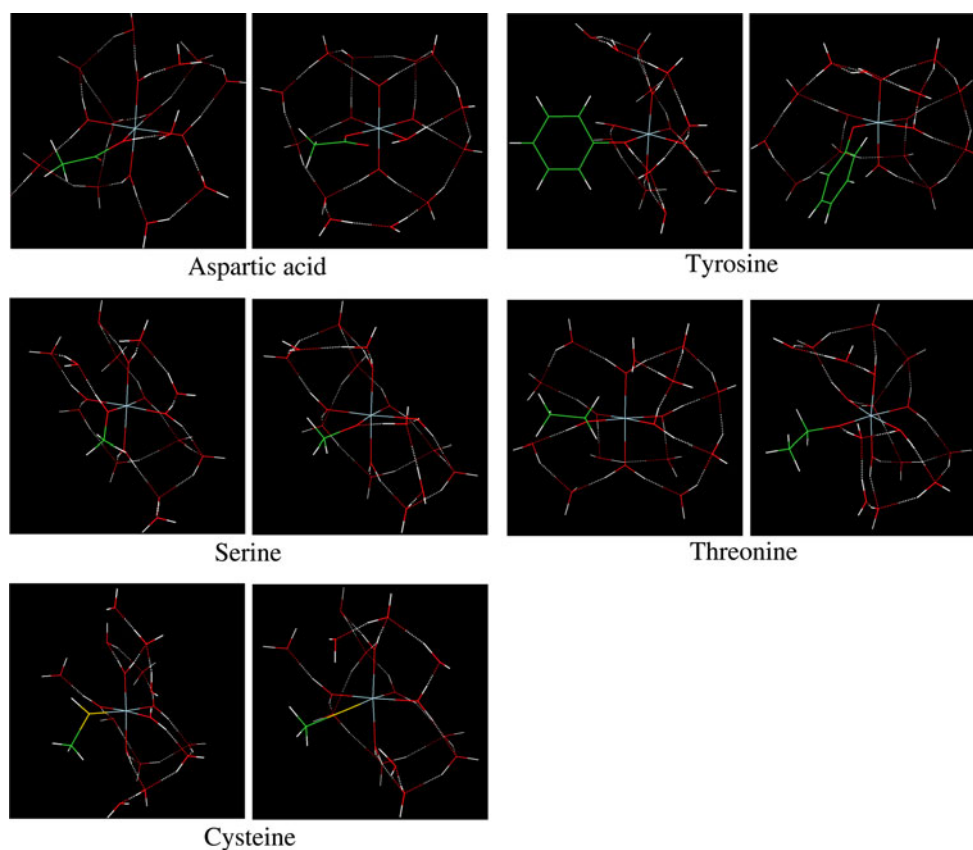
The distances between aluminum and the oxygen atoms of the acidic oxygen atom of each ligand and first solvation water molecules are presented in Table 1. Optimized structures are depicted in Fig. 3. In all the optimized structures, Al(III) presents an octahedral conformation where the ligand is placed in the first solvation sphere and the remaining positions are occupied by water molecules; 12 water molecules are placed in the second hydration sphere.

The protonated ligands (AAH) show neutral charge. In all structures characterized, a hydrogen bond interaction is found between the OH group of the ligand and a second shell water molecule. The average distance between Al(III) and the O atom of first shell water molecules is ca. 1.92 Å for all amino acids. A larger difference is found in the distance between the cation and protonated O atom of the amino acids. Serine and threonine show the shortest distances (ca. 1.93 Å), tyrosine an intermediate value with a Al(III)–O distance 0.3 Å longer (1.953 Å), while aspartic acid presents the longest distance with 1.989 Å.

The deprotonation of these residues changes the interaction between the cation and the ligand, since there is a larger coulombic interaction between Al(III) and the negatively charged deprotonated ligand. Comparing with the Al(III)–AAH interaction, the Al(III)–O distance has shortened to 1.78–1.87 Å. Now, Tyr, Ser and Thr present very similar bond distances, and Asp shows the longest distance (1.866 Å), 0.08 Å larger than the other residues. The carboxylic group of the Al(III)–Asp complex is forming a hydrogen bond between the unbound oxygen atom of the ligand and a first shell water molecule (see Fig. 3). This interaction is not possible for the other amino acids and instead they form a hydrogen bond between the unique oxygen atom of the ligand and a second shell water molecule. On the other hand, the average distances between the first shell water molecules and Al(III) found in the complexes formed by Tyr, Ser and Thr are 1.96 Å, ca. 0.3 Å longer than in the complex formed by their protonated species. The reduction of the total charge of the complex from +3 to +2 may explain this behavior. The average Al(III)– O_w distance in the Al(III)–Asp complex is 1.92 Å, only 0.1 Å longer.

The complex formed by cysteine resembles the complex formed by serine, its analogous O-amino acid, although the Al(III)–S distance is ca. 0.6 Å longer. Again, the distance between Al(III) and the acidic S atom is 0.2 Å longer when it is protonated. The larger Al(III)–S distance in comparison with the Al(III)–O distance does not influence the position of the first shell water molecules, and the average

Fig. 3 B3LYP/6-31++G(d,p) optimized structures of the complexes formed by Al(III) and the amino acids considered in this work: Asp, Tyr, Ser, Thr and Cys. On the left, the neutral AAH specie is presented, and the unprotonated negatively charge AA^- form on the right. Similar structures were obtained with Mg(II)



Al–O_w distance in the complexes formed by the protonated and unprotonated cysteine does not vary from the one shown by serine.

3.1.2 pK_a values

The solution reaction free energies (ΔG_{aq}) computed for each ligand according to Eq. 1, and the estimated pK_a values are shown in Table 1. The standard pK_a values in solution of the related amino acids are also included in the table. Taking into account the values of the pK_a values in solution, Asp is the most acidic amino acid with a pK_a value of 3.9, while the remaining amino acids present significantly higher pK_a values: 8.3 for cysteine, 10.1 for tyrosine and 13.0 for serine and threonine. The ΔG_{aq} presented in Table 1 are negative for Asp, Tyr, Ser and Cys, where Asp presents the largest value (–21.4 kcal/mol), followed by Ser and Thr (–2.2 and –2.3 kcal/mol) and Tyr (–0.9 kcal/mol). Thr is the only amino acid with a positive ΔG_{aq} value (0.8 kcal/mol). These negative values imply that the proton transfer from the amino acid to an Al(III)-bound hydroxide molecule is exoergic and therefore these amino acids are more acidic than the reference water molecule. As a result, their pK_a values are lower than the experimental pK_a value of the Al(III)-bound water molecule (5.0). Asp presents

the lowest pK_a value (–10.7), followed by cysteine (3.3), serine (3.4), tyrosine (4.1) and threonine (5.6). Therefore, the trend in acidity among the different ligands is in general maintained as in solution. The only exception is serine, which unlike in solution, it shows lower pK_a values than tyrosine and threonine. As expected, the interaction with Al(III) has lowered the pK_a value of all ligands. However, the decrease is not the same for all ligands: Asp presents the most significant drop of its pK_a value with a lowering of 14.6 units while for the remaining amino acids the lowering is less drastic, with a decrease in the range of 3–6 units.

3.2 Magnesium complexes

In order to compare the pK_a values obtained for Al(III) complexes with a prototype metal cation prone to Al(III) substitution, similar complexes were characterized for Mg(II) cation. This metal cation is similar in size to Al(III), but with a lower charge, and therefore, these calculations will allow us to perform interesting comparisons to highlight the changes in acidity due to the inclusion of a trivalent cation such as Al(III) in biological environments. We now comment briefly on the results obtained for Mg(II) cation.

Table 1 Reaction free energies of Eq. 1 (ΔG_{aq}) and pK_a values computed for Asp, Tyr, Ser, Thr and Cys interacting with Al(III) and Mg(II). The standard pK_a values of these amino acids are also presented. In addition, the distances between the cation and O atom of the amino acids and the average distances between the cation and the first solvation water molecule's O atom are shown for the unprotonated (AA^-) and protonated (AAH) species

| | Aspartic acid | Tyrosine | Serine | Threonine | Cysteine |
|--|---------------|----------|-------------------------------------|--------------------------------------|----------|
| $\text{pK}_a^{\text{Sol.}}$ (exp.) | 3.9 | 10.1 | 13.0 | 13.0 | 8.3 |
| Aluminum ^a | | | | | |
| Al(III)–O _{AAH} | 1.989 | 1.953 | 1.928 | 1.925 | 2.524 |
| Al(III)–O _{AA⁻} | 1.866 | 1.779 | 1.789 | 1.789 | 2.340 |
| Al(III)–O _{AAH} ^W | 1.920 | 1.919 | 1.924 | 1.926 | 1.918 |
| Al(III)–O _{AA⁻} ^W | 1.932 | 1.955 | 1.958 | 1.960 | 1.956 |
| ΔG_{aq} | –21.4 | –0.9 | –2.2 | 0.8 | –2.3 |
| pK_a^{Al} | –10.7 | 4.1 | 3.4 | 5.6 | 3.3 |
| $\Delta \text{pK}_a^{\text{Al}}$ | 14.6 | 6.0 | 9.6 | 7.4 | 5.0 |
| Magnesium ^b | | | | | |
| Mg(II)–O _{AAH} | 2.201 | 2.169 | 2.105 | 2.104 | 2.749 |
| Mg(II)–O _{AA⁻} | 2.097 | 2.009 | 2.058 | 2.052 | 2.572 |
| Mg(II)–O _{AAH} ^W | 2.096 | 2.093 | 2.105 | 2.107 | 2.095 |
| Mg(II)–O _{AA⁻} ^W | 2.110 | 2.132 | 2.123 | 2.123 | 2.128 |
| ΔG_{aq} | –18.3 | –6.4 | –3.5 ^c /1.6 ^d | –2.0 ^c /3.2 ^d | –5.8 |
| pK_a^{Mg} | –1.0 | 7.7 | 9.8 ^c /13.6 ^d | 10.9 ^c /14.8 ^d | 8.1 |

^a $\text{pK}_a^{\text{exp.}} = 5.0$ [27]

^b $\text{pK}_a^{\text{exp.}} = 12.4$ [41]

^c Spontaneous proton transfer from a second shell water molecule to the unprotonated specie

^d O^W–H^W distance frozen

3.2.1 Structures

All Mg(II) complexes present an octahedral arrangement and they show similar structures to the ones displayed by Al(III) (Fig. 3). The Mg(II)–O and average Mg(II)–O_w distances for these compounds are presented in Table 1. The substitution of a trivalent cation such as Al(III) by the divalent Mg(II) lengthens the distances with respect to the ligand in about 0.2 Å. This elongation is observed for all complexes characterized, including the structures formed by protonated and unprotonated ligands. In spite of this difference, the same trend observed with Al(III) complexes is repeated with Mg(II). Therefore, the neutral protonated amino acids show longer Mg(II)–O distances than their unprotonated counterparts. Moreover, the average Mg(II)–O_w distances are slightly shorter when the amino acid is neutral. However, in the case of unprotonated ligands, not all structures characterized adopted the desired final geometry. In the case of Ser and Thr, the optimization led to a spontaneous proton transfer from a second shell water molecule to the ligand, not observed with Al(III). This proton migration make unrealistic the calculation of pK_a ascribed to the protonation/deprotonation of the ligand oxygen, since in both neutral and negatively charged

species this ligand remains protonated. Therefore, the calculations were repeated with the proton forced to remain bound to the second shell water molecule, freezing the corresponding O^W–H^W distance. The pK_a values obtained with both type of structures are shown in Table 1. But these values should therefore be taken with care.

3.2.2 pK_a values

The computed pK_a values for the Mg(II)-bound amino acids are presented in Table 1. For Asp, Tyr and Cys, the ΔG_{aq} values for the proton transfer from Mg(II) complexes to the Mg(II) bound hydroxide ion are negative. Asp shows the largest (absolute) value (–18.3 kcal/mol), and as with Al(III), the influence of a cation such as Mg(II) lowers the pK_a value of these amino acids studied with respect to their standard values in solution. Tyr also shows a negative ΔG_{aq} value (–6.4 kcal/mol), which is more negative than with Al(III). Note that a more exoergic proton transfer reaction to the reference molecule does not mean that the Mg(II)-bound tyrosine is more acid, as the larger pK_a values of the Mg(II)-bound tyrosine demonstrates. However, the results for Ser and Thr should be analyzed with care. The same behavior as for the rest of the ligands is

found if the fully optimized structures (but those in which the initially unprotonated ligand receives a proton from a water molecule) are considered. However, if we take into account structures partially optimized to force the unprotonated state of the ligands, positive reaction energies are found and we obtain the counter-intuitive results of a higher pK_a for these ligands when interacting with Mg(II) than in solution. Probably the right results is somewhere in between the two estimated values. In general, the pK_a shift observed with Mg(II) is significantly smaller than with Al(III). Asp shows the lowest pK_a value (−1.0), followed by tyrosine (7.7), serine (9.8/13.6) and threonine (10.9/14.8). Finally, the acidity of the cysteine is almost unaltered by the cation, and its pK_a value (8.1) is only 0.2 lower.

4 Discussion

The influence of the trivalent cations Al(III) in the acidity of oxygen-containing side chain amino acids have been quantified by calculating the pK_a of these residues when they are coordinated to Al(III). To estimate the pK_a value, we have applied a protocol based on the calculation of the relative acidity of the residues with respect to an Al(III)-bound water molecule.

First, the accuracy of the method has been measured by comparing the experimental and computational pK_a of a water molecule interacting with Al(III), considering an isolated hydroxide molecule as the basic molecule. If only the first solvation sphere of the hydrated Al(III) complex is considered, a poor result is obtained. However, when the second solvation sphere is explicitly treated by adding 12 water molecules, the value of the pK_a improves, yielding a value of 4.6, in very good agreement with the experimental value of 5.0 [27] and in noticeably support of the results of Yang et al. [28]. Thus, these results confirm what it has extensively pointed out in the literature [23], that the implicit treatment of the solvent by continuum dielectric models it is not sufficient to describe the short-range charge-transfer effects between the cation and water molecules in the vicinity, when highly charged metals are considered. Therefore, the inclusion of explicit water molecules at the second hydration sphere was seen to be key to yield accurate pK_a evaluations.

Since the deprotonation of a water molecule coordinated to the metal was chosen as reference, amino acids with an acidic OH group were included in the study, that is, Asp, Tyr, Ser and Thr. Besides, these amino acids are among the most prone ones to Al(III) interaction. Due to the chemical similarity between oxygen and sulfur, Cys was also studied. From our results, it is clear that Al(III) has a big influence on the acidity of these amino acids, and we can

predict important shifts in the pK_a of these amino acid side chains when coordinated to Al(III). In particular, our data suggests that Asp would show the largest pK_a drop, going from 3.9 units in solution to −10.7 when interacts with Al(III). The other amino acids show also much lower pK_a values: Tyr from 10.1 to 4.1, Ser from 13.0 to 3.4, Thr from 13.0 to 5.6 and Cys from 8.3 to 3.3. Our results also confirm the idea that the interaction of these residues with Al(III) could provoke a change in the protonation state of the neutral residues treated in this work (Tyr, Ser, Thr, and Cys), since all of them show pK_a 's lower than typical physiological pH values. The chemical importance of such shift should not be underestimated, since a change in the protonation state of a given amino acid can lead to important changes in the structure and function of proteins in which Al(III) would be inserted.

In order to compare the differential effect of Al(III) insertion in a metal ion site, we have decided to re-calculate the pK_a 's for a metal such as Mg(II). This metal cation is of similar size to Al(III), but has a lower charge of +2, and it is thought to be a metal particularly prone to Al(III) substitution. The differential effects of these two metal ions on the acidity of the selected side chains of this work will shed light on the effect that may be expected from a highly charged trivalent cation such as Al(III). When Mg(II) is considered, there is also, in general, an increase in the acidity of these residues (lower pK_a 's), but the lowering of these pK_a 's is significantly less pronounced than in the Al(III) case: Asp (−1.0), Tyr (7.7), Cys (8.1), Ser(9.8/13.6) and Thr (10.9/14.8). However, for the amino acids that are neutral at standard conditions (Tyr, Cys, Ser and Thr) the shift in their pK_a 's is not sufficient as to become deprotonated at physiological pH's upon interaction with Mg(II). This is in contrast to the behavior highlighted above for Al(III) and points to a major effect of Al(III)/Mg(II) substitution at the Mg(II) metal binding sites.

5 Concluding remarks

Aluminum is a non-essential element that has been introduced recently in the human body. Al(III) has been seen to enter binding sites of several enzymes that should be filled up by other metals, such as magnesium [42]. The higher positive charge of Al(III) triggers geometrical changes in the protein, such as shorter metal-ligand distances. In the present work, we have quantified the effect that Al(III) insertion would have in the acidity of oxygen-containing side chains bound to the metal. The present study confirms that the acidity of these amino acids coordinated to Al(III) suffers a drastic increase (lower pK_a 's), which could provoke deprotonation of neutral side chains such as Tyr, Ser, Thr or Cys at physiological pH's. This deprotonation is

much less likely to occur when residues are bound to a divalent metal ion such as Mg(II), and therefore, this could be an important difference in the chemical behavior of Al(III)/Mg(II) amino acids, and constitutes one key factor to consider when explaining disruption of protein functionality upon Al(III)/Mg(II) substitution [43]. Our results allow for a quantification of these effects through the accurate evaluation of the shift in pK_a 's upon Al(III) coordination.

Acknowledgments This research was funded by Eusko Jaurlaritz (the Basque Government) and the Spanish MCyT. The SGI/IZO-SGIker UPV/EHU is acknowledged for computational resources.

References

1. Exley C (2003) *J Inorg Biochem* 97:1–7
2. Exley C, Esiri MM (2006) *J Neurol Neurosurg Psychiatry* 77:877–879
3. Macdonald TL, Martin RB (1988) *Trends Biochem Sci* 13:15–19
4. Ganrot PO (1986) *Environ Health Perspect* 65:363–441
5. Martin RB (1986) *Clin Chem* 32:1797–1806
6. Collery P, Pirer L, Manfait F, Etienne J (1990) In: Alzheimer's disease and dementia syndromes consecutive to imbalanced mineral metabolisms subsequent to blood brain barrier alteration. John Libbey-Eurotext
7. Trapp GA (1980) *Neurotoxicology* 1:89–100
8. Nehru B, Bhalla P, Garg A (2006) *Mol Cell Biochem* 290:33–42
9. Xu ZX, Fox L, Melethil S, Winberg L, Badr M (1990) *J Pharm Exp Ther* 254:301–305
10. Ravi SM, Prabhu BM, Raju TR, Bindu PN (2000) *J Physiol Pharmacol* 44:473–478
11. Yang X, Zhang Q, Li L, Shen R (2007) *J Inorg Biochem* 101:1242–1250
12. Nishimasu H, Fushinobu S, Shoun H, Wakagi T (2007) *J Biol Chem* 282:9923–9931
13. Juffer AH (1998) *Biochem Cell Biol* 76:198–209
14. Ho JM, Coote ML (2010) *Theor Chem Acc* 125:3–21
15. Saracino GAA, Improta R, Barone V (2003) *Chem Phys Lett* 373:411–415
16. Topol IA, Tawa GJ, Caldwell RA, Eissenstat MA, Burt SK (2000) *J Phys Chem A* 104:9619–9624
17. Chipman DM (2002) *J Phys Chem A* 106:7413–7422
18. Liptak MD, Shields GC (2001) *J Am Chem Soc* 123:7314–7319
19. Dong HT, Du HB, Qian XH (2008) *J Phys Chem A* 112:12687–12694
20. Magill AM, Cavell KJ, Yates BF (2004) *J Am Chem Soc* 126:8717–8724
21. Takano Y, Houk KN (2005) *J Chem Theory Comput* 1:70–77
22. Ho JM, Coote ML (2009) *J Chem Theory Comput* 5:295–306
23. Martinez JM, Pappalardo RR, Marcos ES, Mennucci B, Tomasi J (2002) *J Phys Chem B* 106:1118–1123
24. Pliego JR, Riveros JM (2002) *J Phys Chem A* 106:7434–7439
25. Kelly CP, Cramer CJ, Truhlar DG (2006) *J Phys Chem A* 110:2493–2499
26. Bickmore BR, Tadanier CJ, Rosso KM, Monn WD, Eggett DL (2004) *Geochim Cosmochim Acta* 68:2025–2042
27. Sposito G (1995) *The environmental chemistry of aluminium*. CRC, Boca Raton
28. Yang WJ, Qian ZS, Miao Q, Wang YJ, Bi SP (2009) *Phys Chem Chem Phys* 11:2396–2401
29. Rezabal E, Mercero JM, Lopez X, Ugalde JM (2007) *Chem Phys Chem* 8:2119–2124
30. Lopez X, Schaefer M, Dejaegere A, Karplus M (2002) *J Am Chem Soc* 124:5010–5018
31. Mujika JI, Mercero JM, Lopez X (2003) *J Phys Chem A* 107:6099–6107
32. Frisch MJ, Trucks GW, Schlegel HB, Scuseria GE, Robb MA, Cheeseman JR, Montgomery JA Jr, Vreven T, Kudin KN, Burant JC, Millam JM, Iyengar SS, Tomasi J, Barone V, Mennucci B, Cossi M, Scalmani G, Rega N, Petersson GA, Nakatsuji H, Hada M, Ehara M, Toyota K, Fukuda R, Hasegawa J, Ishida M, Nakajima T, Honda Y, Kitao O, Nakai H, Klene M, Li X, Knox JE, Hratchian HP, Cross JB, Bakken V, Adamo C, Jaramillo J, Gomperts R, Stratmann RE, Yazyev O, Austin AJ, Cammi R, Pomelli C, Ochterski JW, Ayala PY, Morokuma K, Voth GA, Salvador P, Dannenberg JJ, Zakrzewski VG, Dapprich S, Daniels AD, Strain MC, Farkas O, Malick DK, Rabuck AD, Raghavachari K, Foresman JB, Ortiz JV, Cui Q, Baboul AG, Clifford S, Cioslowski J, Stefanov BB, Liu G, Liashenko A, Piskorz P, Komaromi I, Martin RL, Fox DJ, Keith T, Al-Laham MA, Peng CY, Nanayakkara A, Challacombe M, Gill PMW, Johnson B, Chen W, Wong MW, Gonzalez C, Pople JA (2004) *Gaussian 03 revision C 02*. Gaussian Inc., Wallingford
33. Becke AD (1993) *J Chem Phys* 98:5648–5652
34. Becke AD (1988) *Phys Rev A* 38:3098–3100
35. Lee C, Yang W, Parr RG (1988) *Phys Rev B* 37:785–789
36. Vosko SH, Wilk L, Nusair M (1980) *Can J Phys* 58:1200–1211
37. Barone V, Cossi M, Tomasi J (1998) *J Comput Chem* 19:404–417
38. Barone V, Cossi M, Tomasi J (1997) *J Chem Phys* 107:3210–3221
39. Cossi M, Barone V, Cammi R, Tomasi J (1996) *Chem Phys Lett* 255:327–335
40. Cancès E, Mennucci B, Tomasi J (1997) *J Chem Phys* 107:3032–3041
41. Douglas B, McDaniel D, Alexander J (1994) *Concepts and models of inorganic chemistry*. Wiley, New York
42. Exley C (2009) *Trends Biochem Sci* 34:589–593
43. Glick JL (1991) *J Theor Biol* 148:283–286